Available online at www.sciencedirect.com
ScienceDirect
Remote Sensing of Environment 109 (2007) 464–472
Remote Sensing of Environment
www.elsevier.com/locate/rse

Remote chlorophyll-*a* retrieval in turbid, productive estuaries: Chesapeake Bay case study

Anatoly A. Gitelson [a,*], John F. Schalles [b], Christine M. Hladik [c,1]

[a] *Center for Advanced Land Management Information Technologies (CALMIT), School of Natural Resources, University of Nebraska-Lincoln, Lincoln, NE 68588-0517, USA*
[b] *Biology Department, Creighton University, Omaha, NE 68178-0103, USA*
[c] *Environmental Science Institute, Florida A&M University, Tallahassee, FL 32307, USA*

Received 10 November 2006; received in revised form 23 January 2007; accepted 27 January 2007

Abstract

Accurate remote assessment of phytoplankton chlorophyll *a* (chl*a*) concentration is particularly challenging in turbid, productive waters. Recently a conceptual model containing reflectance in three spectral bands in the red and near infra-red range of the spectrum was suggested for retrieving chl*a* concentrations in turbid productive waters; it was calibrated and validated in lakes and reservoirs in Nebraska and Iowa. The objective of this paper is to evaluate the performance of this three band model as well as its special case, the two-band model to estimate chl*a* concentration in Chesapeake Bay, as representative of estuarine Case II waters, and to assess the accuracy of chl*a* retrieval. To evaluate the model performance, dual spectroradiometers were used to measure subsurface spectral radiance reflectance in the visible and near infra-red range of the spectrum. Water samples were collected concurrently and contained widely variable chl*a* (9 to 77.4 mg/m^3) and total suspended solids (7–65 mg/L dry wt). Colored dissolved organic matter (CDOM) absorption at 440 nm was 0.20 to 2.50 m^{-1}; Secchi disk transparency ranged from 0.28 to 1.5 m. The two- and three-band models were spectrally tuned to select the spectral bands for most accurate chl*a* estimation. Strong linear relationships were established between analytically measured chl*a* and both the three-band model $[R^{-1}(675)–R^{-1}(695)]\times R(730)$ and the two-band model $R(720)/R(670)$, where $R(\lambda)$ is reflectance at wavelength λ. The three-band model accounted for 81% of variation in chl*a* and allowed estimation of chl*a* with a root mean square error (RMSE) of less than 7.9 mg/m^3, whereas the two-band model accounted for 79% of chl*a* variability and RMSE of chl*a* estimation was below 8.4 mg/m^3. The three-band model with MERIS spectral bands allows accurate chl*a* estimation with RMSE below 9.1 mg/m^3. Two-band model with SeaWiFS bands and MODIS 667 nm and 748 nm bands can estimate chl*a* with RMSE below 11 mg/m^3. The findings underlined the rationale behind the conceptual model and demonstrated the robustness of this algorithm for chl*a* retrieval in turbid, productive estuarine waters.

Keywords: Reflectance; Chlorophyll; Model

1. Introduction

Remote sensing is an effective tool for synoptic monitoring of ecosystem health. Even a few images are useful as aids in the design or improvement of point sampling programs, often through highlighting the best locations and timing for sampling. The techniques are based on relationships between reflectance $R(\lambda)$ and two inherent optical properties (IOPs), total absorption (a) and backscattering (b_b) coefficients (e.g., Gordon et al., 1988):

$$R(\lambda)\propto\gamma\frac{b_b(\lambda)}{a(\lambda)+b_b(\lambda)} \quad (1)$$

where γ is dependent on the geometry of the light field emerging from the water body. Historically, remote sensing of

* Corresponding author.
E-mail address: Gitelson@calmit.unl.edu (A.A. Gitelson).
[1] Current address: Department of Marine Sciences, University of Georgia, Athens, GA 30602-3636, USA.

0034-4257/$ - see front matter © 2007 Elsevier Inc. All rights reserved.
doi:10.1016/j.rse.2007.01.016

chlorophyll *a* concentration (chl*a*) used the blue and the green spectral regions (e.g., Gordon & Morel, 1983) and was confined to open ocean Case I waters (Morel & Prieur, 1977). Attempts to apply Case I derived algorithms to Case II productive waters (Morel & Prieur, 1977), containing widely variable and poorly correlated chl*a*, suspended solids, and dissolved organic matter concentrations resulted in poor predictive ability (e.g., Dall'Olmo et al., 2005; GKSS, 1986; Gons, 1999; Schalles, 2006). In productive turbid waters absorption by dissolved organic matter, tripton, and phytoplankton pigments in the blue spectral region overlap, and prevents using this region for chl*a* retrieval. In many estuaries, tripton and CDOM dominate water column optics. For example, phytoplankton accounted, on average, for only about 5% of vertical attenuation in San Francisco Bay (Cole & Cloern, 1987).

To quantify chl*a* in productive turbid waters, a variety of algorithms have been developed; all are based on the properties of the reflectance peak near 700 nm (e.g., Gitelson, 1992; Gitelson & Kondratyev, 1991; Schalles, 2006). These include the ratio of the reflectance peak (R_{max}) to the reflectance at 670 nm (R_{670}), or the ratio R_{705}/R_{670} (Dekker, 1993; Gitelson, 1992; Gitelson & Kondratyev, 1991); the position of this peak (Gitelson, 1992). Gons (1999) used the reflectance ratio at 704 and 672 nm and absorption and backscattering coefficients at these wavelengths to assess chl*a* concentrations ranging from 3 to 185 mg/m^3. Alternatively, good correlations have been found between chl*a* and the band ratio R_{725}/R_{675} (Dall'Olmo & Gitelson 2005; Hoge et al., 1987; Pierson & Strvmbeck, 2000; Ruddick et al., 2001; Yacobi et al., 1995).

All these methods are based on the assumption that optical parameters such as the chl*a* specific absorption coefficient, $a^*_{chla}(\lambda)$, and the chl*a* fluorescence quantum yield, η, remain constant. In reality, these parameters depend on the physiological state and structure of the phytoplankton community and can vary widely (e.g., Bricaud et al., 1995) Fluorescence quantum yield is affected by phytoplankton taxonomic composition, illumination conditions, light adaptation, nutritional status, and temperature and can vary by eight-fold (e.g., Fischer & Kronfeld, 1990; GKSS, 1986). Therefore, the assumptions of constant a^*_{chla} and η can be a significant source of uncertainty in algorithms for remote chl*a* estimation. IOPs may thus be spatially and temporally heterogenous, and it may be necessary to define and measure specific IOPs for a specific time and place (e.g., Brando & Dekker, 2003). This consideration is particularly important for procedures using inversion models to estimate chl*a* from water reflectance.

Recently, Dall'Olmo et al. (2003) provided empirical evidence that a three-band reflectance model, originally developed for estimating pigment contents in terrestrial vegetation (Gitelson et al., 2003a, 2005), could also be used to assess chl*a* in turbid productive waters in the form:

$$Chla \propto [R^{-1}(\lambda_1) - R^{-1}(\lambda_2)] \times R(\lambda_3) \quad (2)$$

where $R(\lambda_i)$ is reflectance in spectral band λ_i.

For productive turbid waters, the absorption coefficient in the denominator of Eq. (1) is a sum of the absorption coefficients of chl*a*, colored dissolved organic matter (CDOM), tripton (non-algal particles) and water:

$$a = a_{chla} + a_{tripton} + a_{CDOM} + a_{water} \quad (3)$$

To retrieve chl*a* concentration, one needs to isolate the chl*a* absorption coefficient, a_{chla}. To accomplish that, reciprocal reflectance in the first spectral band λ_1 (Eq. (2)) should be maximally sensitive to a_{chla}, i.e., to be restricted to a range of 660 to 690 nm (Dall'Olmo & Gitelson, 2005). However, in turbid productive waters in addition to absorption by chl*a*, $R^{-1}(\lambda_1)$ might also be strongly affected by absorption of tripton, CDOM, and water as well as backscattering b_b by all particulate matter. The effect of $(a_{tripton}+a_{CDOM})$ and b_b (in denominator of Eq. (1)) could be minimized using a second spectral band where $R^{-1}(\lambda_2)$ is least sensitive to the absorption by chl*a* ($a_{chla}(\lambda_2) \ll a_{chla}(\lambda_1)$ and absorption coefficients of tripton and CDOM ($a_{tripton}+a_{CDOM}$) at λ_2 are quite close to that in band λ_1.

The difference $R^{-1}(\lambda_1)-R^{-1}(\lambda_2)$ in Eq. (2), however, is still affected by b_b (in numerator of Eq. (1)), so model estimations for the same chl*a* value would differ if backscattering varies between samples. To account for the variability in scattering between samples, it was suggested using a third spectral band λ_3, where reflectance is minimally affected by the absorption of constituents, $(a_{chla}+a_{tripton}+a_{CDOM}) \sim 0$, and thus, $a(\lambda_3) \sim a_w$. The near-infrared (NIR) range beyond 710 nm, where $a \gg b_b$ and $R_{NIR} \propto b_b$, meets the above requirements.

The two-band model (Gitelson et al., 1985)

$$Chla \propto R^{-1}(\lambda_1) \times R(\lambda_3) \quad (4)$$

is a special case of the conceptual model (Eq. (2)) when $a_{chla}(\lambda_1) \gg b_b(\lambda_1)$, and $a_{chla}(\lambda_1) \gg a_{tripton}(\lambda_1)+a_{CDOM}(\lambda_1)$ (Dall'Olmo & Gitelson, 2005).

Calibration and validation of the models in Eqs. (2) and (4) were done using a large set of experimental observations in lakes and reservoirs in Nebraska and Iowa which exhibited widely variable optical properties (Dall'Olmo & Gitelson, 2005).

Variability of the chl*a* fluorescence quantum yield and, especially, of the chl*a* specific absorption coefficient considerably reduce the accuracy of remote chl*a* estimation. To minimize these effects, the authors proposed tuning the model band positions rather than simply parameterize the model's coefficients. Optimal locations of spectral bands were found, in accordance with the optical properties of the study sites. Although the large range of the optically active constituents sampled helped validate the robustness of the model, the model was based on conditions in inland waters and never evaluated in estuarine and coastal Case 2 waters. Schalles (2006) compared the utility of a number of published Case 1 and Case 2 algorithms for chl*a* estimating in coastal waters, and found that many lacked robustness or simply did not apply to the optically complex coastal conditions.

We focused on optically complex Chesapeake Bay waters (e.g., Gallegos et al., 2005; Gallegos & Neale, 2002; Magnuson et al., 2004; Tzortziou et al., 2007) with complicated

phytoplankton, particulate matter and CDOM dynamics (e.g., Fisher et al., 1988; Harding et al., 2005). The objectives of the present study were (a) to evaluate the utility of the three band conceptual model (Dall'Olmo & Gitelson, 2005) and its special case two band model (Dall'Olmo & Gitelson, 2005; Gitelson et al., 1985) for remote estimation of chl*a* in Chesapeake Bay and its tributaries as a typical example of turbid, Case II estuarine waters, and (b) to assess the potential accuracy of chl*a* retrieval from remotely sensed data.

2. Methods and techniques

To assess the applicability of the models (Eqs. (2) and (4)) and its accuracy, field studies were conducted between July 11 and July 18, 2005 at 44 stations on the Maryland reach of Chesapeake Bay and a set of tributary rivers varying in length, discharge regimes, and watershed land covers and loadings (Fig. 1). Stations were selected to provide assessment of the model performance over a wide range of water column optical conditions. All measurements and water samplings were made within 3.5 h of solar noon (solar noon — 13:12 EDST), and 75% of our measurements were within 2 h of solar noon. At each station, the following were measured: downwelling irradiance, upwelling radiance, Secchi disk transparency (m), salinity (psu), temperature (°C), depth (m), and coordinates of latitude and longitude (Fig. 1). Bulk water samples were collected near surface by bucket bailing and transferred to 10 l polyethylene containers. Samples were placed in the shade. Morning samples were transferred to a shore team and afternoon samples returned directly to the laboratory. At the lab, samples were refrigerated and processed within 6 h of collection.

Our measurements were made on board a 5.5 m Creighton University Sundance Skiff with special provisions for optical work. Radiance reflectance measurements were made with a

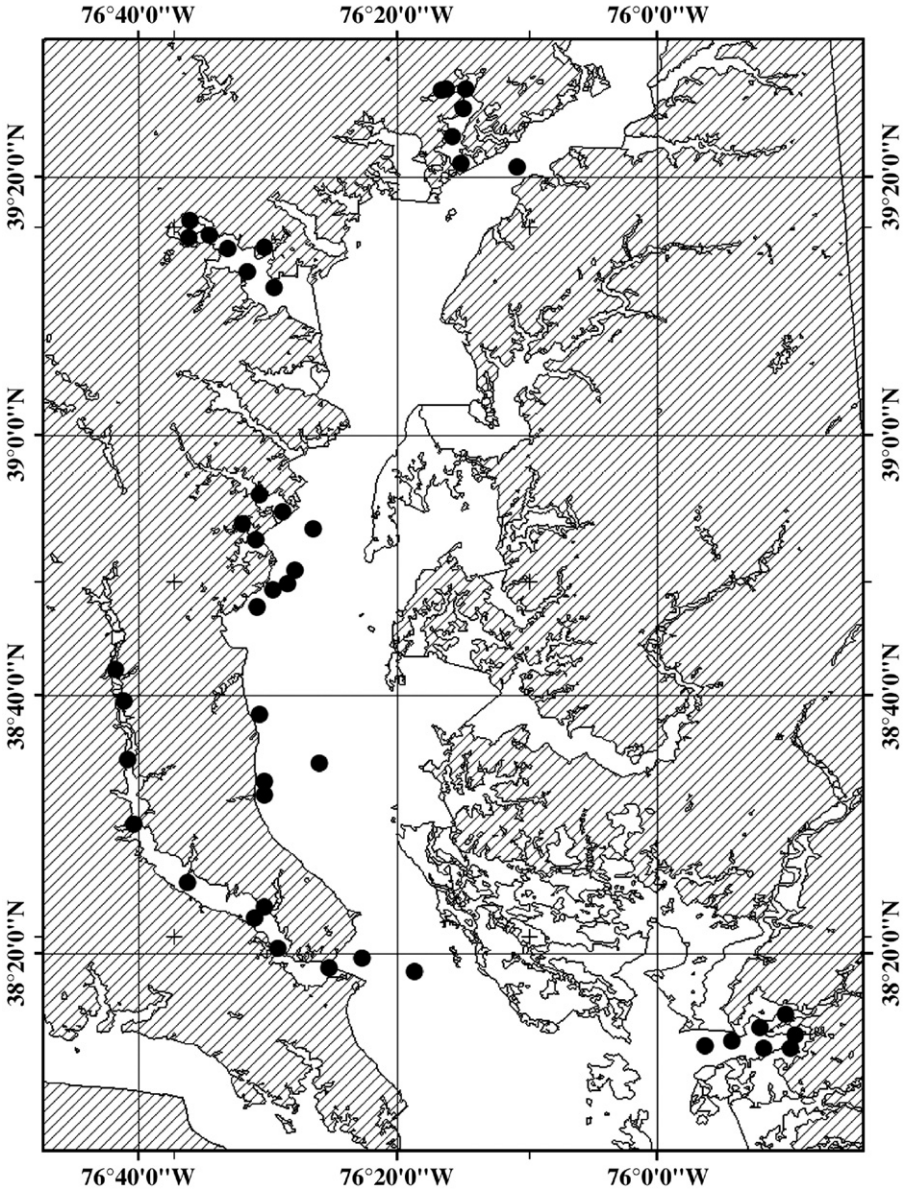

Fig. 1. Map of sampling stations in Chesapeake Bay, July 11–18, 2005.

dual optical fiber system, with two inter-calibrated Ocean Optics USB2000 radiometers (350–1000 nm range, with a sampling interval of ~0.3 nm and a spectral resolution of ~1.5 nm). Radiometer 1, equipped with a 25° field-of-view, 10 m optical fiber, measured the upwelling radiance of water (L_{up}). Radiometer 2, equipped with an optical fiber and cosine diffuser (yielding a hemispherical field of view), was pointed upward to simultaneously measure incident irradiance (E_{inc}). Downwelling signal was captured with a 3 m fiber optic cable with cosine collector mounted on an unshaded, 2.5 m mast. Readings of upwelling radiance were taken with the fiber end mounted on a hand held pole, and the probe tip submerged about 5 cm. To match the transfer functions of the radiometers, intercalibration of the instruments was accomplished by measuring the upwelling radiance (L_{cal}) of a white Spectralon reflectance standard (Labsphere, Inc., North Sutton, NH) simultaneously with incident irradiance (E_{cal}) measured by the downwelling sensor. Percentage reflectance was computed as:

$$R(\lambda) = [L(\lambda)_{up}/E(\lambda)_{inc}] \times [E(\lambda)_{cal}/L(\lambda)_{cal}] \times 100 \times R(\lambda)_{cal}$$

where $R(\lambda)_{cal}$ is the reflectance of the Spectralon panel linearly interpolated to match the band centers of each radiometer (detail in Dall'Olmo & Gitelson, 2005). Data collection and management were performed using a data management program, CDAP, written by Mr. B. Leavitt, CALMIT, University of Nebraska-Lincoln.

The critical issue with regard to the dual-fiber approach is that the transfer functions of both radiometers should be identical. Using the same instrument configuration, we studied the identity of two radiometers and confirmed that the coefficient of variation of the ratio of the transfer functions of the two radiometers does not exceed 0.4% (Dall'Olmo & Gitelson, 2005). Wavelength to channel calibrations of the two instruments used in this study are performed at a CALMIT optical calibration facility at the University of Nebraska. The instruments have proven very stable over time, and changes in the polynomial equation coefficients which describe the wavelength to channel relationship are very subtle.

Water samples were processed under subdued lighting. Duplicate measures were made for chl*a*, total suspended solids (TSS), and CDOM. Average values for each replicate pair are reported. Aliquots of the bulk samples were filtered through glass fiber filters (Whatman 47 mm GF/C). Chlorophyll pigment was extracted using 10 mL of 90% acetone buffered with $MgCO_3$ and macerated with a tissue grinder. The extracted samples were filtered through glass fiber filters and filtrate absorbance at 750, 664, 647, and 630 nm was determined using 1 cm cuvettes and a Geneysis 5 spectrophotometer (Spectronics, Inc.). Chl*a*, with no acidification procedure for phaeophytin, was estimated using the trichromatic equation (APHA, 1998). TSS was determined gravimetrically using pre-ashed and tared filters. Filters and retained particulate matter were dried (60 °C for at least 24 h) and reweighed. CDOM absorption was estimated using second filtrate fractions (first fractions discarded) from the TSS procedure. Absorption of filtrate at 440 nm was measured with a 10 cm quartz cuvette and Geneysis 5 spectrophotometer. Absorption estimates were converted to m^{-1}.

3. Results

Widely variable water column conditions were encountered (mean values and ranges): TSS = 16.5 (7.0–64.8 mg/L dry weight), CDOM absorption at 440 nm = 0.75 (0.20–2.50 m^{-1}), Secchi disk depth = 0.80 (0.28 to 1.50 m), salinity 7.4 (0.1–12.0 PSU), and water depth = 7.3 (0.95–25.2 m). Our ranges of constituent values appear typical for the Maryland section of Chesapeake Bay and its tributaries (e.g., Fisher et al., 1988; Magnuson et al., 2004; Tzortziou et al., 2007 and references therein). Our measured Chl*a* ranged between 9 and 77.4 mg/m^3 with a mean value of 30 mg/m^3 and a median of 25 mg/m^3. Minimal Chl*a* concentrations in our data set were greater than minimal chl*a* observed at some seasons in Upper Bay (1 mg/m^{-3}), Mid Bay (4.3 mg/m^3) and Lower Bay (2.2 mg/m^3) (Magnuson et al., 2004; Tzortziou et al., 2007).

Chl*a* concentration and TSS were not related (Fig. 2, determination coefficient of linear relationship $r^2 < 0.0015$). Clearly chl*a* was not the only characteristic controlling water optical properties, confirming that these were Case 2 waters (Morel & Prieur, 1977).

Reflectance was highly variable over the visible and NIR spectral regions (Fig. 3; spectral range of 400–800 nm displayed). The spectra were quite similar in magnitude to typical reflectance spectra collected in turbid productive waters (Dall'Olmo & Gitelson, 2005; Gitelson et al., 2000; Lee et al., 1994; Schalles, 2006). While reflectance in the range from 400 nm to about 470 nm remained below 2%, reflectance in the green range was much higher, reaching 5%, and the peak around 700 nm at many stations was nearly the same in magnitude as the green reflectance peak. NIR reflectance was below 2% and widely variable. The variation of reflectance was minimal in the blue range (see spectrum of standard deviation of reflectance: thick line in Fig. 3). The minimum near 440 nm,

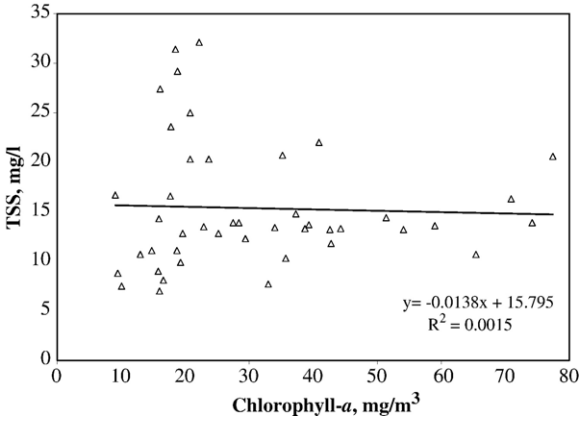

Fig. 2. Total suspended solids concentrations plotted versus chlorophyll *a* concentrations. The concentrations of these constituents varied independently, thus, the waters studied are typical case II waters.

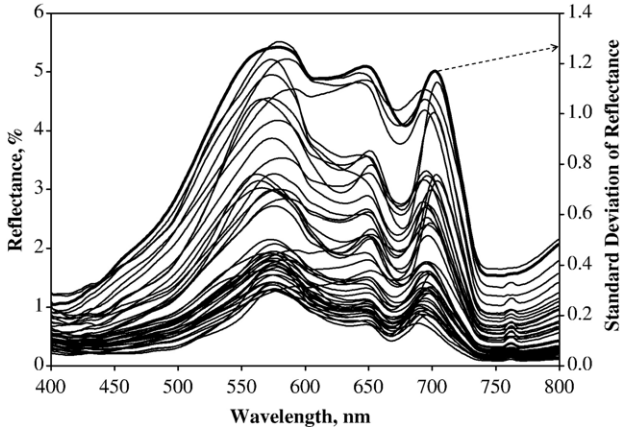

Fig. 3. Reflectance spectra and standard deviation of reflectance in Chesapeake Bay.

corresponding to chl*a* absorption, was almost indistinct in the reflectance spectra and reflectance in the range 400 to 500 nm did not have pronounced spectral features over the broad range of turbidity and chl*a* concentration. Absorption by dissolved organic matter and tripton, and scattering by particulate matter contributed strongly to reflectance patterns in this spectral range and, as a result, the blue to green ratio R_{440}/R_{550} (e.g., Gordon & Morel, 1983) was poorly related to chl*a* and appears inadequate for estimating chl*a* in these waters (Fig. 4, $r^2 < 0.24$, root mean square error (RMSE) of chl*a* estimation, RMSE = 15.87 mg/m^3).

In the green range around 550 nm, absorption by pigments was minimal and scattering by all particulate matter played the main role in reflectance. Reflectance in this range varied about five-fold with variations in the concentration and composition of constituents. Reflectance had a prominent peak around 700 nm; in this spectral range, chl*a* absorption decreases with wavelength while absorption by pure water increases. Thus, the peak manifests minimal combined absorption by all constituents (e.g., Gitelson, 1992; Gitelson et al., 1986; Vasilkov & Kopelevich, 1982; Vos et al., 1986). As in other productive turbid waters, the reflectance peak position shifts toward longer wavelengths with increasing chl*a*, from 688 nm when chl*a* was 9 mg/m^3 to about 706 nm for chl*a* above 70 mg/m^3. Chl*a* was very poorly related to peak magnitude; chl*a* was responsible for only 2% of peak magnitude variation (not shown). This suggests that scattering by inorganic and non-living organic suspended matter played a critical role, and largely controlled reflectance in this spectral region.

As with the peak magnitude, chl*a* was very poorly related to the reflectance in the range of chl*a* red absorption around 670 nm (it was responsible only for 3% change in R_{670}), showing that beside absorption by chl*a*, reflectance in this range was strongly affected by absorption and scattering by other constituents.

Thus, to accurately retrieve chl*a* from reflectance data, it is critical to subtract the effects of other constituents on reflectance around 670 nm as suggested in the conceptual models (Eqs. (2) and (4)). In order to find optimal positions of spectral bands, we

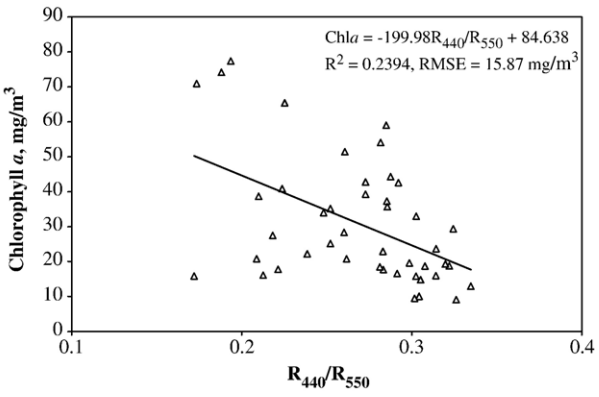

Fig. 4. Chlorophyll *a* concentration versus blue-to-green ratio for Chesapeake Bay in July 2005.

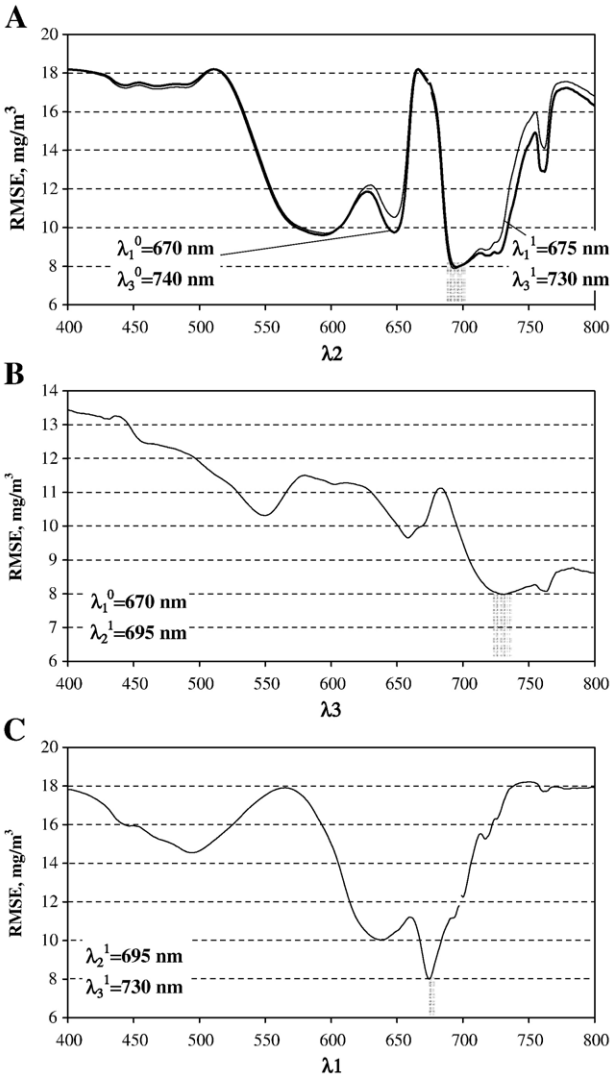

Fig. 5. RMSE error of chl*a* estimation by the model Eq. (2) when one wavelength is varied between 400 nm and 800 nm. A: Finding optimal λ_2^1 with initial λ_1^0 and λ_3^0 (thick curve); B: finding optimal λ_3^1 with initial λ_1^0 and λ_2^1 (thick curve); C: finding optimal λ_1^1 with λ_2^1 and λ_3^1. In forth step (thin curve in figure A) we tested whether λ_2^1 that has been found with initial λ_1^0 and λ_3^0 was really optimal. Optimal wavebands have been found as: $\lambda_1 = 675$ nm, $\lambda_2 = 695$ nm and $\lambda_3 = 730$ nm.

Table 1
Slopes (m) and intercepts (n) of the relationship "chl$a$ versus Model" with corresponding root mean square error of chl$a$ estimation (RMSE, in mg/m^3) and coefficient of determination (r^2)

Models	m	n	r^2	RMSE
MODIS R_{440}/R_{550}	−199.98	84.63	0.24	15.87
MODIS $R_{678}^{-1}\times R_{748}$	125.4	−2.95	0.51	12.7
MODIS $R_{667}^{-1}\times R_{748}$	147.0	−10.91	0.65	10.7
SeaWiFS $R_{670}^{-1}\times R_{765}$	150.0	−16.49	0.68	10.4
MERIS $(R_{665}^{-1}-R_{708}^{-1})\times R_{750}$	194.2	18.77.5	0.75	9.1
$R_{673}^{-1}\times R_{735}$	121.4	−11.70	0.69	10.1
$R_{665}^{-1}\times R_{725}$	73.6	−14.74	0.73	9.4
$R_{675}^{-1}\times R_{705}$	44.1	−26.44	0.78	8.5
$(R_{671}^{-1}-R_{710}^{-1})\times R_{740}$	165.5	24.85	0.79	8.35
$R_{670}^{-1}\times R_{720}$	59.8	−17.55	0.79	8.39
$(R_{675}^{-1}-R_{695}^{-1})\times R_{730}$	178.9	10.14	0.81	7.9

Number of samples N=44.

tuned the model (Eq. (2)) and its special case, the two-band model (Eq. (4)) in accord with optical properties of the medium.

3.1. Three-band model tuning

In the first step, we used initial positions for λ_1^0=670 nm and λ_3^0=740 nm in Eq. (2) to find the first approximation for position of λ_2 (λ_2^1). The λ_1^0 was chosen within the range of maximum chl$a$ absorption, the λ_3^0 was in the NIR range where scattering controls reflectance. We regressed the model $[R^{-1}(670)–R^{-1}(\lambda_2)]\times R(740)$ vs. chl$a$ for the range of 400 to 800 nm and found a minimal RMSE of chl$a$ estimation for λ_2 around 695 nm (Fig. 5A, thin line).

In the second step, we found a first approximation of λ_3^1, after fixing λ_2^1=695 nm and regressing the model $[R^{-1}(670)–R^{-1}(695)]\times R(\lambda_3)$ vs. chl$a$. The RMSE was minimal in a rather wide range of λ_3 around 730 nm (Fig. 5B).

In the third step, we found a first approximation of λ_1 (λ_1^1), regressing the model $[R^{-1}(\lambda_1)–R^{-1}(695)]\times R(730)$ vs. chl$a$. The RMSE was minimal for λ_1^1=675 nm. Fixing λ_1^1=675 nm and λ_3^1=730 nm, we found finally that λ_2^1=695 nm remained the optimal wavelength for our data set (Fig. 5A, thin line). Thus, we have found optimal spectral bands for chl$a$ estimation using the three-band model:

$$\text{chl}a = 178.9 \times [R^{-1}(675)-R^{-1}(695)] \times R(730) + 10.14 \quad (5)$$

Maximal determination coefficient r^2>0.81 and minimal RMSE of chl$a$ estimation (below 7.9 mg/m^3) was achieved using a three-band model with spectral bands λ_1=674–676 nm, λ_2=691–698 nm, and λ_3=723–739 nm. RMSE below 8.5 mg/m^3 could be obtained with bands 672–678 nm, 689–707 nm and 712–769 nm and RMSE below 9 mg/m^3 with bands 671–680 nm, 688–720 nm and 705–780 nm.

3.2. Two-band model tuning

To find the optimal spectral bands λ_1 and λ_3 in the two-band model Eq. (4), we used the same approach as described above for the three-band model. *In the first step*, with initial λ_1^0=675 nm (chl$a$ absorption maximum) we found λ_3^1=720 nm. *In the second step* fixing λ_3^1, we found λ_1^1=670 nm. *In the third step* we tested whether λ_3^1 as found in the third step is really optimal. We regressed $R^{-1}(670)\times R(\lambda_3)$ vs. chl$a$, and the minimal RMSE of chl$a$ estimation was again found at λ_3=720 nm, so $\lambda_3^2=\lambda^1{}_3$. Thus, we have found optimal spectral bands for chl$a$ estimation using the two-band model:

$$\text{chl}a = 59.8 \times R^{-1}(670) \times R(720) - 17.55 \quad (6)$$

Maximal determination coefficient r^2>0.79 and minimal RMSE of chl$a$ estimation (below 8.39 mg/m^3) was achieved using Eq. (6) with spectral bands λ_1=668–672 nm, and λ_3=713–722 nm. RMSE below 9 mg/m^3 could be obtained with spectral bands 666–675 nm and 707–729 nm.

Several ocean color sensors are provided with channels in red and NIR spectral regions. To evaluate performance of the models with spectral bands of satellite sensors, the field data collected in this study were averaged over the bandwidth of these sensors. Medium Resolution Imaging Spectrometer (MERIS) has the red spectral bands (center/width) 665/10 nm and 705/10 nm as well as the NIR band 754/8 nm. The three-band model with MERIS spectral bands allows accurate chl$a$ estimation with RMSE below 9.1 mg/m^3. The Sea Wide Field-of-View Sensor (SeaWiFS) has one red band (center/width)

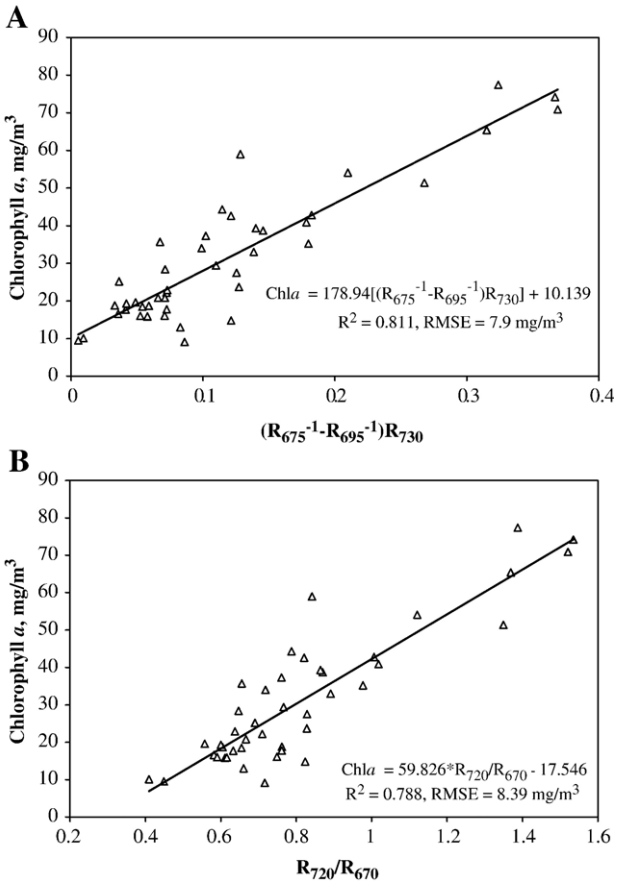

Fig. 6. Three-band (A) and two-band (B) models (Eqs. (5) and (6)) plotted versus analytically measured chlorophyll-a concentrations.

670/20 nm and NIR band 765/40 nm. The Moderate Imaging Spectrometer (MODIS) has two closely located red bands, 667/9.5 nm and 678/9 nm and NIR band 748/10 nm. Thus, the two-band model could potentially use SeaWiFS and MODIS data (Dall'Olmo et al., 2005). Two-band model with SeaWiFS bands and MODIS 667 nm and 748 nm bands allows estimate chl*a* with RMSE below 11 mg/m^3 (Table 1). The two-band model with MODIS 678 nm and 748 nm bands was less accurate (RMSE < 12.7 mg/m^3), as it was previously found for US inland waters (Fig. 6 in Dall'Olmo et al., 2005).

4. Discussion

Having identified the optimal spectral bands for both models (Eqs. (5) and (6)), we evaluated the performance of (a) the two- and three-band models with spectral bands that were found to be optimal for US turbid productive inland waters (Dall'Olmo & Gitelson, 2006), and (b) the two-band model $R_{675}^{-1}\times R_{705}$ that is widely used for chl*a* estimation in inland waters (e.g., Gitelson, 1992; Gitelson et al., 1985) — Table 1. The iterative band tuning for Chesapeake Bay only slightly improved the performance of the three-band model compared with the initial band positions found for US inland waters (λ_1=671 nm, λ_2=710 nm, λ_3=740 nm; Dall'Olmo & Gitelson 2005): with RMSE values of 7.9 mg/m^3 vs. 8.35 mg/m^3 (Table 1). *Thus, to accurately estimate chla in estuarine waters as in Chesapeake Bay the three-band inland water model did not require further optimization of spectral band positions*.

The two-band model optimized for US inland waters, $R_{673}^{-1}\times R_{735}$ and $R_{665}^{-1}\times R_{725}$ (Dall'Olmo & Gitelson, 2005) was also accurate for Chesapeake Bay-RMSE of chl*a* estimation below 10 mg/m^3 (Table 1). *Thus, the two-band model also did not require further optimization of spectral band positions*.

The two-band model $R_{675}^{-1}\times R_{705}$ with bands 673–677 nm and 703–708 nm had almost the same accuracy (RMSE=8.5 mg/m^3) as the two-band model optimized for these waters (8.39 mg/m^3). The much better performance of this model in Chesapeake Bay compared to that in US inland waters (Dall'Olmo & Gitelson, 2005) can be explained by the fact that maximal chl*a* concentrations in Chesapeake Bay were much lower than in the US lake and reservoir data set (around 80 mg/m^3 in Chesapeake Bay vs. 200 mg/m^3 in reservoirs), thus, absorption by chl*a* at λ_3=705 nm was very low and $R(\lambda_3)$ was governed mainly by backscattering of all particulate matter. As in the original formulation of this two-band model (λ_1=675 nm and λ_3=705 nm, Gitelson et al., 1985), it allowed accurate estimation at low to moderate chl*a* concentrations.

Findings in this paper are in accord with the results of sensitivity analysis of two- and three-band models (Dall'Olmo & Gitelson, 2006) and the conclusions retrieved from analysis of an extended data set obtained over US inland waters with widely variable optical properties (Dall'Olmo & Gitelson, 2005). They found that for both two- and three-band models, the RMSE had a minimum at λ_1 between 660 and 673 nm, where the models are least sensitive to variation in $a^*_{\mathrm{chl}a}$ between samples. In Chesapeake Bay maximal accuracy was also achieved for λ_1 in this spectral range. Dall'Olmo and Gitelson (2005) found that maximal RMSE occurred in a narrow range of λ_1 near 685 nm, where the algorithms are strongly affected by variability in quantum yield of chl*a* fluorescence. For Chesapeake Bay data, a shift in λ_1 from 667 nm to a longer wavelength (680 nm) resulted in a sharp increase in RMSE (compare performance of two MODIS models $R_{678}^{-1}\times R_{748}$ and $R_{667}^{-1}\times R_{748}$ presented in Table 1).

In the conceptual model Eq. (2), $R^{-1}(\lambda_2)$ was used to account for variations in the a_{tripton}, a_{CDOM} and b_{b} (in denominator of Eq. (1)), whereas $R^{-1}(\lambda_3)$ was used to account for variations in b_{b} (in the numerator of Eq. (1)). Dall'Olmo and Gitelson (2005) reported that the optimal spectral regions λ_2 and λ_3 for US inland waters overlapped between 730 and 750 nm. In that case, the effect of the variability in the backscattering coefficient on reflectance was greater than the variability of tripton and dissolved organic matter absorption. By contrast, Chesapeake Bay data showed that an optimal λ_2 occurs within a narrow range near 710 nm, while the optimum for λ_3 is near 730 nm. Thus, in Chesapeake Bay waters the variability in absorption by tripton and dissolved organic matter concentrations were significant factors. Therefore, λ_2, in a narrow range, should be used to account for the effect of these constituents. To verify this hypothesis, further study of dissolved organic matter and tripton absorption in these and other estuarine and coastal waters is needed.

It is noteworthy that the three-band model with spectral bands optimized for inland waters with chl*a* ranging from 4.4 to 217.3 mg/m^3 (Dall'Olmo & Gitelson, 2005) allowed accurate estimation of chl*a* when applied to Chesapeake Bay, in spite of having a very different composition of optically active constituents (chl*a*, tripton, CDOM). Also, the model worked robustly despite differences in the taxonomy of phytoplankton in bloom states at some of our Chesapeake Bay and tributary stations. At some stations, cyanobacteria were quite dominant, at others dinoflagellates were dominant, and some stations had mixed assemblages (unpublished data from Richard Lacouture, Chunlei Fan, and Pat Tester). The models used in this study do not require data on inherent optical properties of constituents — these can be variable and difficult to obtain. Instead, tuning spectral band positions of the model minimized the effect of variability in bio-optical parameters and increased the accuracy of chl*a* estimation. Additionally, the cost associated with hand-held radiometers and their ease of use offers widespread applications for monitoring as the diverse conditions of coastal and inland waters.

The same conceptual model (Eq. (2)) has been used for non-destructive pigment retrieval from reflectance spectra of plant leaves (anthocyanins: Gitelson et al., 2001; carotenoids: Gitelson et al., 2002; chlorophyll: Gitelson et al., 2003a), fruit peels (Merzlyak et al., 2003), total chlorophyll content and biomass in crops (Gitelson et al., 2003b, 2005) as well as chl*a* retrieval in inland turbid productive waters (Dall'Olmo & Gitelson, 2005, 2006; Dall'Olmo et al., 2003) and in hypereutrophic waters with chl*a* above 3000 mg/m^3 (Zimba & Gitelson, 2006). This study brings additional evidence that the conceptual model may be considered as a unified approach for remote quantification of constituent concentrations in a variety of systems.

The algorithms featured in this paper were tuned to a very seasonally-limited *in situ* data set obtained in July, 2005. It remains to be determined how well these algorithms perform in estuarine waters during other seasons and other locations where the expected relative contributions to absorption and scattering by sediments, CDOM and phytoplankton varies from the conditions captured during the July 2005 sampling.

Acknowledgements

This research was supported partially by NASA grant NNG06GA92G to Tom Fisher (Horn Point Lab., University of Maryland) and Anatoly Gitelson and by a subcontract to John Schalles and Don Rundquist of NOAA grant NA17AE1624 to Larry Robinson (Environmental Science Institute, Florida A&M University). The following individuals assisted in field measurements and laboratory analysis: Andrew Binderup, Robert Carlson, Lea Chasar, Edward Cizek, Kevin Dillon, Chunlei Fan, Chris Holland, Alex Gilerson, Richard Lacouture, Megan Machmuller, Joel Mulder, Susan Pasko, and Latrincy Whitehurst. Laboratory facilities and other logistical support were generously provided by Kelly Clark at Morgan State University's Estuarine Research Center and by Julie Bortz at the Maryland Department of Natural Resources' Otter Point Creek unit of the Maryland National Estuarine Research Reserve. Sam Ahmed, Robert Carlson, Mark Harwell, Richard Lacouture, and Pat Tester all contributed to planning, logistical support, and conceptual discussions for this study. We thank Galina Keydan (UNL) for assistance in data processing and three anonymous reviewers for the helpful comments. A contribution of the University of Nebraska Agricultural Research Division, Lincoln, NE, Journal Series No. 15010. This research was also supported in part by funds provided through the Hatch Act.

References

American Public Health Association. (1998). *Standard methods for the examination of water and wastewater.* Section 1200 — chlorophyll (20th ed.). American Public Health Association.

Brando, V. E., & Dekker, A. G. (2003). Satellite hyperspectral remote sensing for estimating estuarine and coastal water quality. *IEEE Transactions on Geoscience and Remote Sensing*, *41*, 1378−1387.

Bricaud, A., Babin, M., Morel, A., & Claustre, H. (1995). Variability in the chlorophyll-specific absorption coefficients of natural phytoplankton: Analysis and parameterization. *Journal of Geophysical Research [Oceans]*, *100*, 13321−13322.

Cole, B. E., & Cloern, J. E. (1987). An empirical model for estimating phytoplankton productivity in estuaries. *Marine Ecology. Progress Series*, *36*, 299−305.

Dall'Olmo, G., & Gitelson, A. A. (2005). Effect of bio-optical parameter variability on the remote estimation of chlorophyll-*a* concentration in turbid productive waters: Experimental results. *Applied Optics*, *44*, 412−422.

Dall'Olmo, G., & Gitelson, A. A. (2006). Effect of bio-optical parameter variability and uncertainties in reflectance measurements on the remote estimation of chlorophyll-a concentration in turbid productive waters: Modeling results. *Applied Optics*, *45*, 3577−3592.

Dall'Olmo, G., Gitelson, A. A., & Rundquist, D. C. (2003). Towards a unified approach for remote estimation of chlorophyll-*a* in both terrestrial vegetation and turbid productive waters. *Geophysical Research Letters*, *30*, 1038. doi:10.1029/2003GL018065

Dall'Olmo, G., Gitelson, A. A., Rundquist, D. C., Leavitt, B., Barrow, T., & Holz, J. C. (2005). Assessing the potential of SeaWiFS and MODIS for estimating chlorophyll concentration in turbid productive waters using red and near-infrared bands. *Remote Sensing of Environment*, *96*, 176−187.

Dekker, A. (1993). Detection of the optical water quality parameters for eutrophic waters by high resolution remote sensing. PhD Thesis, Free University, Amsterdam, The Netherlands.

Fisher, T. R., Harding, Jr., L. W., Stanley, D. W., & Ward, L. G. (1988). Phytoplankton, nutrients and turbidity in the Chesapeake, Delaware and Hudson estuaries. *Estuarine, Coastal and Shelf Science*, *27*, 61−93.

Fischer, J., & Kronfeld, V. (1990). Sun-stimulated chlorophyll fluorescence: 1. Influence of oceanic properties. *International Journal of Remote Sensing*, *11*, 2125−2147.

Gallegos, C. L., Jordan, T. E., Hines, A. H., & Weller, D. E. (2005). Temporal variability of optical properties in a shallow, eutrophic estuary: Seasonal and interannual variability. *Estuarine, Coastal and Shelf Science*, *64*, 156−170.

Gallegos, C. L., & Neale, P. J. (2002). Partitioning spectral absorption in case 2 waters: Discrimination of dissolved and particulate components. *Applied Optics*, *41*, 4220−4233.

Gitelson, A. A. (1992). The peak near 700 nm on reflectance spectra of algae and water: Relationships of its magnitude and position with chlorophyll concentration. *International Journal of Remote Sensing*, *13*, 3367−3373.

Gitelson, A. A., Gritz, U., & Merzlyak, M. N. (2003). Relationships between leaf chlorophyll content and spectral reflectance and algorithms for non-destructive chlorophyll assessment in higher plant leaves. *Journal of Plant Physiology*, *160*, 271−282.

Gitelson, A. A., Yacobi, Y. Z., Schalles, J. F., Rundquist, D. C., Han, L., Stark, R., et al. (2000). Remote estimation of phytoplankton density in productive waters. *Archiv für Hydrobiologie Special Issues Advance Limnology*, *55*, 121−136.

Gitelson, A., Keydan, G., & Shishkin, V. (1985). Inland waters quality assessment from satellite data in visible range of the spectrum. *Soviet Remote Sensing*, *6*, 28−36.

Gitelson, A., Nikanorov, A. M., Sabo, G., & Szilagyi, F. (1986). Etude de la qualite des eaux de surface par teledetection. *IAHS Publication*, *157*, 111−121.

Gitelson, A. A., & Kondratyev, K. Y. (1991). Optical models of mesotrophic and eutrophic water bodies. *International Journal of Remote Sensing*, *12*, 373−385.

Gitelson, A. A., Merzlyak, M. N., & Chivkunova, O. B. (2001). Optical properties and non-destructive estimation of anthocyanin content in plant leaves. *Photochemistry and Photobiology*, *74*(1), 38−45.

Gitelson, A. A., Viña, A., Arkebauer, T. J., Rundquist, D. C., Keydan, G., & Leavitt, B. (2003). Remote estimation of leaf area index and green leaf biomass in maize canopies. *Geophysical Research Letters*, *30*, 1248. doi:10.1029/2002GL016450

Gitelson, A. A., Viña, A., Ciganda, V., Rundquist, D. C., & Arkebauer, T. J. (2005). Remote estimation of canopy chlorophyll content in crops. *Geophysical Research Letters*, *32*, L08403. doi:10.1029/2005GL022688

Gitelson, A. A., Zur, Y., Chivkunova, O. B., & Merzlyak, M. N. (2002). Assessing carotenoid content in plant leaves with reflectance spectroscopy. *Photochemistry and Photobiology*, *75*(3), 272−281.

Gons, H. J. (1999). Optical teledetection of chlorophyll *a* in turbid inland waters. *Environmental Science & Technology*, *33*, 1127−1132.

Gordon, H. R., Brown, O. B., Evans, R. H., Brown, J. W., Smith, R. C., Baker, K. S., et al. (1988). A semianalytic radiance model of ocean color. *Journal of Geophysical Research*, *93*, 10909−10924.

Gordon, H., & Morel, A. (1983). Remote assessment of ocean color for interpretation of satellite visible imagery. A review. *Lecture notes on coastal and estuarine studies*, *Vol. 4*. Springer-Verlag.

GKSS. (1986). The use of chlorophyll fluorescence measurements from space for separating constituents of sea water. ESA Contract No. RFQ3-5059/84/NL/MD Vol II, GKSS, Research Centre, Germany.

Harding, Jr., L. W., Magnuson, A., & Mallonee, M. E. (2005). SeaWiFS retrieval of chlorophyll in Chesapeake Bay and the mid-Atlantic bight. *Estuarine, Coastal and Shelf Science*, *62*, 75−94.

Hoge, E. F., Wright, C. W., & Swift, R. N. (1987). Radiance ratio algorithm wavelengths for remote oceanic chlorophyll determination. *Applied Optics*, *26*, 2082−2094.

Lee, Z. P., Carder, K. L., Hawes, S. K., Steward, R. G., Peacock, T. G., & Davis, C. O. (1994). Model for the interpretation of hyperspectral remote-sensing reflectance. *Applied Optics*, *33*, 5721−5732.

Magnuson, A., Harding, Jr., L. W., Mallonee, M. E., & Adolf, J. E. (2004). Bio-optical model for Chesapeake Bay and the middle Atlantic bight. *Estuarine, Coastal and Shelf Science*, *61*, 403−424.

Merzlyak, M. N., Solovchenko, A. E., & Gitelson, A. A. (2003). Reflectance spectral features and non-destructive estimation of chlorophyll, carotenoid and anthocyanin content in apple fruit. *Postharvest Biology and Technology*, *27*, 197−211.

Morel, A., & Prieur, L. (1977). Analysis of variations in ocean color. *Limnology and Oceanography*, *22*, 709−722.

Pierson, D., & Strvmbeck, N. (2000). A modeling approach to evaluate preliminary remote sensing algorithms: Use of water quality data from Swedish great lakes. *Geophysica*, *36*, 177−202.

Ruddick, K. G., Gons, H. J., Rijkeboer, M., & Tilstone, G. (2001). Optical remote sensing of chlorophyll *a* in case 2 waters by use of an adaptive two-band algorithm with optimal error properties. *Applied Optics*, *40*, 3575−3585.

Schalles, J. F. (2006). Optical remote sensing techniques to estimate phytoplankton chlorophyll *a* concentrations in coastal waters with varying suspended matter and CDOM concentrations. In L. Richardson & E. Ledrew (Eds.), *Remote sensing of aquatic coastal ecosystem processes: Science and management applications* (pp. 27−79). Springer.

Tzortziou, M., Subramaniam, A., Herman, J. R., Gallegos, C. L., Neale, P. J., & Harding Jr., L. W. (2007). Remote sensing reflectance and inherent optical properties in the mid Chesapeake Bay. *Estuarine, Coastal and Shelf Science*, *72*, 16−32.

Vasilkov, A., & Kopelevich, O. (1982). Reasons for the appearance of the maximum near 700 nm in the radiance spectrum emitted by the ocean layer. *Oceanology*, *22*, 697−701.

Vos, W. L., Donze, M., & Bueteveld, H. (1986). On the reflectance spectrum of algae in water: The nature of the peak at 700 nm and its shift with varying concentration. *Technical Report. Communication on Sanitary Engineering and water Management, Delft, The Netherlands* (pp. 86−92).

Yacobi, Y. Z., Gitelson, A., & Mayo, M. (1995). Remote sensing of chlorophyll in Lake Kinneret using high spectral resolution radiometer and Landsat TM: Spectral features of reflectance and algorithm development. *Journal of Plankton Research*, *17*, 2155−2173.

Zimba, P. V., & Gitelson, A. A. (2006). Remote estimation of chlorophyll concentration in hyper-eutrophic aquatic systems: Model tuning and accuracy optimization. *Aquaculture*, *256*, 272−286.